DYNAMIC PROPERTIES OF TYPICAL CONSULTATION ROOM MEDICAL COMPONENTS

L. Di Sarno[*a], C. Petrone[b], G. Magliulo[c] and G. Manfredi[d]

[a]*University of Sannio, Department of Engineering, Piazza Roma 21, 82100 Benevento, Italy, ldisarno@unisannio.it*

[b]*University of Naples Federico II, Department of Structures for Engineering and Architecture, via Claudio 21, 80125 Naples, Italy, crescenzo.petrone@unina.it*

[c]*University of Naples Federico II, Department of Structures for Engineering and Architecture, via Claudio 21, 80125 Naples, Italy, gmagliul@unina.it*

[c]*University of Naples Federico II, Department of Structures for Engineering and Architecture, via Claudio 21, 80125 Naples, Italy, gamanfre@unina.it*

ABSTRACT

The dynamic response of typical components of a consultation room in hospital buildings is investigated through full-scale shake table tests. Low-intensity random vibration tests were carried out on two freestanding medical cabinets and a desk. The natural frequency and the damping ratio of the components are evaluated via standardized methods.

Simplified finite element models of the tested components are implemented in order to assess whether simplified models can adequately describe the dynamic behavior of medical components. The outcomes of the numerical analyses fairly match the results obtained from the experimental tests. It is demonstrated that simple models are able to adequately simulate the dynamic properties of sample medical components and can be employed in the earthquake response analysis of healthcare facilities.

KEYWORDS: nonstructural components, shake table test, dynamic identification, natural frequency, damping, hospital building contents, finite element model

[*] L.Di Sarno. University of Sannio Department of Engineering, Piazza Roma 21, 82100 Benevento, Italy, ldisarno@unisannio.it, , tel. +39 0824 305566, fax. +39(0)824 325246.

1 Introduction

The failure of nonstructural systems, especially hospital building contents and services, represents about 80% of the loss exposure of critical buildings to earthquakes (e.g. [1]). It is thus essential to include the response of nonstructural components when assessing the seismic risk of hospitals, building contents and services. The essential functions of the hospitals must remain fully operational for at least 72 hours to provide emergency response when an earthquake occurs, because of the increase of patients to be assisted. Consequently, the damage to structural and nonstructural components and the failure of building contents should be prevented in hospitals. Numerous reconnaissance surveys carried out in the aftermath of major world-wide recent earthquakes demonstrated that large financial losses were caused to health care facilities, especially hospital buildings (e.g. [2-9], among others). For example, the common surveyed damage includes the overturning of bookshelves containing medical files with patient details. Hazardous contaminants may also be released when the bookshelves overturn; hence, there is a number of dangerous consequences caused by the lack of seismic protection, e.g. through restrainers and links to the walls. The connections between the surgery lamps and the slab may be severely damaged during a strong motion shaking. The medical lamps of the surgery rooms are heavy cantilever components, which are clamped to the slab. During the combined horizontal and vertical component of the earthquake ground motions such lamps may experience large oscillations, thus imposing large demands on the connections with the slab. The above connections may fail and, in turn, they impair the functionality of the surgery room.

There are sound procedures to evaluate the structural seismic performance of several building systems; such procedures are implemented in codes of practice (see, for example, [10-13]). However, there is a lack of reliable yet simplified numerical models and adequate seismic analyses to either design or assess the earthquake performance of freestanding medical laboratory nonstructural components. The latter components generally consist of complex sub-assemblages made of either metallic or wooden frames and/or plates. The evaluation of their dynamic response is

not straightforward as it exhibits high nonlinearities; it significantly depends on the friction coefficients of the equipment supports. The mechanical properties of the interface contact, between the heavy medical equipment and the laboratory floors, can be experimentally determined by conducting slow-pull tests on the equipment. Simplified idealizations of the interface contact include elasto-plastic models and the classical Coulomb friction, where static and kinetic friction coefficients are utilized [14]. The static friction coefficient remarkably depends on the type of the pull-force. The kinetic friction coefficient exhibits a pressure and velocity dependence. Sliding, rocking and overturning are the most common failure modes that may affect the response of freestanding medical furniture (e.g. [14-17]). Several seismic codes [18] do not deal with the use of friction for nonstructural components. However, many medical equipment could be hardly used if they were rigidly connected to the floor. For instance, while a cabinet could be fixed to the wall, the desk should remain unrestrained on the floor. An inaccurate approach of the current building codes is therefore evidenced.

Few experimental and numerical studies have been carried out to assess the seismic vulnerability of typical medical equipment [14, 19, 20]. There is however an urgent need to provide an insight into the modal identification of the typical components of hospital buildings.

Towards this aim, a shake table test campaign is carried out to investigate the dynamic response of the most common components of a typical hospital consultation room. Low-intensity random vibration tests are performed on two freestanding cabinets, considering different mass configurations in the cabinets, and a desk. Both the natural frequency and the damping ratio of the components are investigated. Simple finite element models of the tested components are implemented and their dynamic properties are compared with the experimental outcomes. The aim of the paper is to demonstrate that simplified models can adequately simulate the dynamic behavior of medical components for practical use.

2 Experimental evaluation of modal response with shake table tests

The seismic tests on hospital building contents are carried out by the earthquake simulator system available at the laboratory of Structures for Engineering and Architecture Department of University of Naples Federico II, Italy. The system consists of two 3 m x 3 m square shake tables. Each table is characterized by two degrees of freedom along the two horizontal directions.

A steel single-story framed system is designed with the purpose of simulating the seismic effects on the medical contents of a typical hospital room. The test frame is designed in order to simulate the effects of the earthquake ground motion at different floors on a hospital building; its large stiffness prevents the onset of the resonance. The effects of the interstorey drift were not considered, because they are not relevant for the problem at hand. The layout of the model consists of a 2.42 m x 2.71 m x 2.72 m test fixture of S275 steel material with concentric V-bracings. Further details on the steel test setup are included in Magliulo et al. [21].

A typical hospital examination (out patients consultation) room background is reproduced within the sample steel frame. Plasterboard partitions and ceilings are mounted; linoleum sheets are also installed to cover both the floor and a large portion of the internal partitions. An overhead light and a ray film viewer are also installed in the room. The building contents used for the examination room include: (a) a hospital medicine cabinet made of cold formed sheet with dimension 75x38x165 cm, having double moving glass doors with locker and four mobile shelves; (b) a hospital medicine cabinet made of cold formed sheet with dimension 53x36x139 cm, having single moving glass door with locker and four mobile shelves; (c) a desktop computer (monitor, case, keyboard and mouse); (d) a desk made of a steel pipe frames and a wooden desktop. The mass of the two cabinets is respectively 15 kg for the single-window cabinet and 20 kg for the double-window cabinet; the mass of the desk is 31.6 kg. Cabinet contents with different slenderness, as flasks, test tubes, glass beakers and glass bottles, are placed in the cabinets to simulate the actual conditions of a typical hospital room. Different mass distributions are also selected to distribute such contents in the single- and double-window cabinets.

The present experimental research focuses on realistic medical components, i.e. cabinet with shelves loaded with different height-wise weights. A variety of configuration layouts, related to the arrangement of the contents on the different shelves, are experimentally investigated (Table 1).

In test group 1000 the dynamic behavior of the cabinet with an equivalent mass is assessed, i.e. sand inserted in boxes, at each shelf of the cabinets. A 6 kg mass and a 4 kg mass are respectively added for each shelf of the double-window cabinet and of the single-window cabinet (Fig. 1a); the mass amount is representative of the mass of typical contents inserted in such a cabinet. The use of the equivalent mass is required in order to investigate the behavior of the cabinets with different contents on the shelves. The contents are simulated through the use of sand boxes in order to prevent damage and contents replacement after each shaking.

In test group 2000 the dynamic behavior of the cabinets with a decreasing mass distribution along the height is investigated. From the base to the top, 6 kg, 4 kg, 4 kg and 2 kg masses are placed on the four shelves of the double-window cabinet, while 4 kg, 2 kg, 2 kg and 0 kg masses are placed on the four shelves of the single-window cabinet (Fig. 1b). The aim of these tests is to investigate the behavior of cabinets in which, as typically suggested, the heaviest contents are placed at the lowest shelves.

In test group 3000 typical glass contents are tested, as shown in Fig. 1c. The contents are equally placed on the different shelves of each cabinet. Glass bottles with different dimensions, i.e. 100 ml, 250 ml and 500 ml, are placed in the double-window cabinet with 4.40 kg whereas 250 ml and 100 ml flasks, test tubes and glass beakers are placed in the single-window cabinet. They are filled with colored sand, that simulates the presence of water. A 4.40 kg mass is added to each shelf of the double-window cabinet, whereas a 2.03 kg mass is added to each shelf of the single-window cabinet.

Table 1. Test program details.

Test group	Plan configuration	Cabinets contents
1000	1	Equivalent mass uniformly distributed along the height
2000	1	Equivalent mass non uniformly distributed along the height
3000	1	Typical glass contents uniformly distributed along the height
4000	2	Equivalent mass uniformly distributed along the height
5000	2	Equivalent mass non uniformly distributed along the height
6000	2	Typical glass contents uniformly distributed along the height

(a) (b) (c)

Fig. 1. Single-window cabinet in (a) test groups 1000 and 4000, (b) test groups 2000 and 5000 and in (c) test groups 3000 and 6000.

In Fig. 2a the plan configuration of the different components in test groups 1000, 2000 and 3000 is shown, whereas a different plan configuration is defined in test groups 4000, 5000 and 6000 (Fig. 2b). The components are arranged in such a way that the equipment is shaken along the two orthogonal directions, given the unidirectional input motion. In test groups 4000, 5000 and 6000 the same content mass configurations of test groups 1000, 2000 and 3000, respectively, are chosen.

This work will primarily focus on the results carried out by applying random unidirectional excitations. The random vibration tests are performed before shake table tests at increasing intensity, which are detailed in Cosenza et al. [22].

Random vibration inputs are considered in order to dynamically identify the sample components. They are characterized by a large frequency content over a wide frequency range, so that they are capable of exciting different natural modes of the components. For each test group different random

vibration tests are performed, whose ID, acceleration amplitude and root mean square are reported in Table 2.

The low amplitude shakings can be employed to evaluate the influence of the different parameters on the dynamic properties of the nonstructural components, both in terms of natural frequency and damping ratio. The root mean squares of the performed tests are in line with the values suggested by FEMA 461 [23], i.e. 0.05g±0.01g.

The interaction between horizontal and vertical shaking was not considered herein. Such an interaction should be further investigated, especially for those components possessing friction-based restraints.

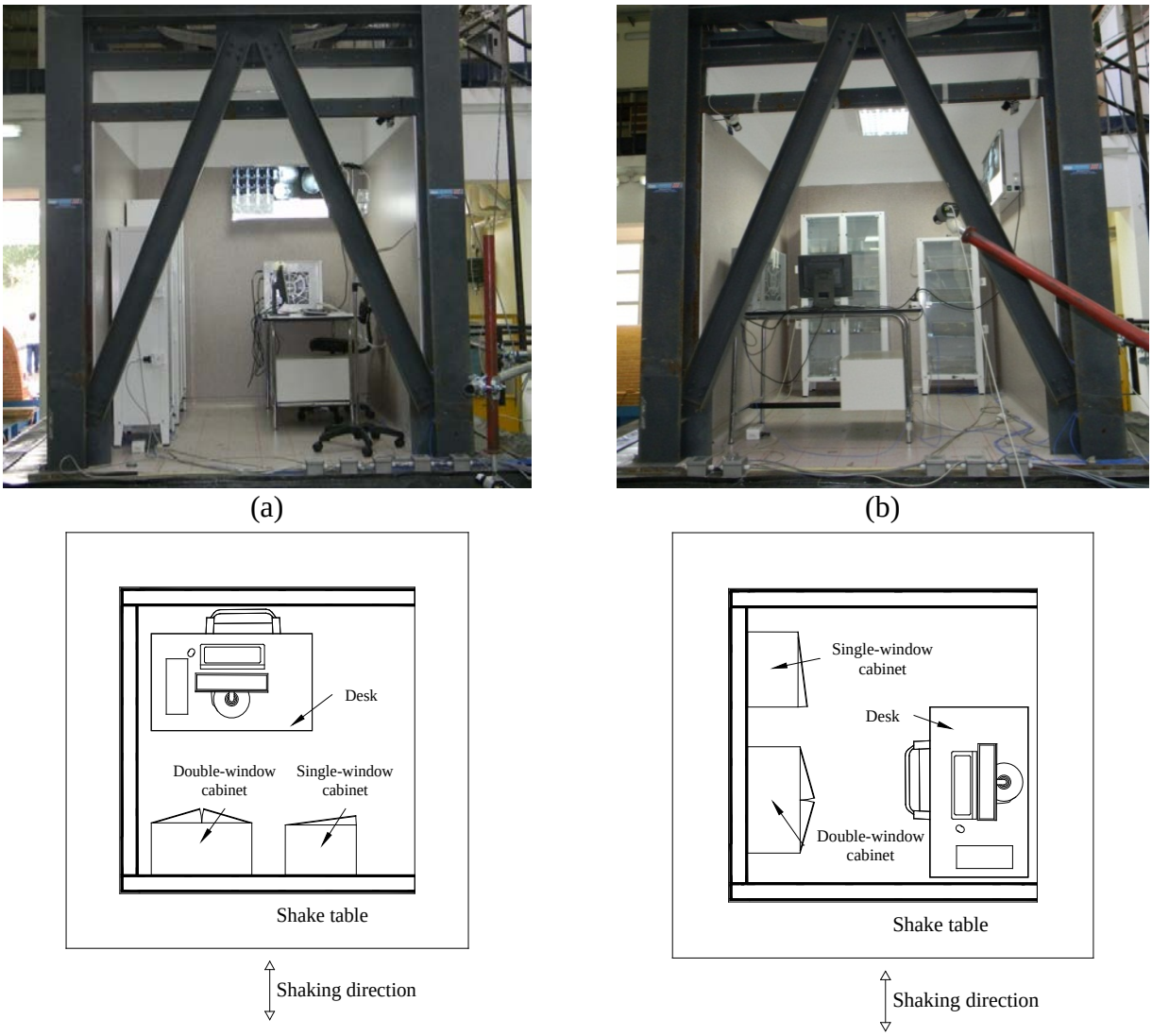

Fig. 2. Photo and plan view of the test setup: (a) and (c) configuration 1, adopted in test groups 1000, 2000 and 3000, and (b) and (d) configuration 2, adopted in test groups 4000, 5000 and 6000.

Table 2. Random vibration tests ID, acceleration amplitude and root mean square.

	Test ID	Amplitude [m/s/s]	Root mean square [m/s/s]
1000	1001	0.54	0.16
	1002	1.09	0.26
	1003	2.12	0.51
	1004	2.66	0.64
2000	2001	1.00	0.27
	2002	1.97	0.48
3000	3000	0.67	0.26
	3001	1.07	0.24
	3002	2.54	0.61
4000	4001	0.97	0.25
	4002	2.10	0.48
5000	5001	1.00	0.27
	5002	2.02	0.48
6000	6001	1.06	0.26
	6002	1.90	0.47

Sine-sweep tests are also carried out; the results of such tests, which reasonably match the outcomes of the random vibration tests, are omitted for the sake of brevity in the present paper.

High quality digital accelerometers are used to monitor the response of the hospital building contents. Four triaxial accelerometers are placed for each of the two cabinets; they are located at the base of each cabinet, i.e. at the lowest shelf level, at the top of the cabinet of the front side and at two intermediate heights (Fig. 3); one accelerometer is placed at the top of the desk, while one accelerometer measures the acceleration at the shake table level. The accelerometers are positioned close to the sides of the cabinets (Fig. 1) in order to minimize the influence of local modes of the thin steel plates. The accelerometer recording could be affected by torsion mechanism in the cabinets. The sampling frequency of the accelerometers is equal to 400 Hz.

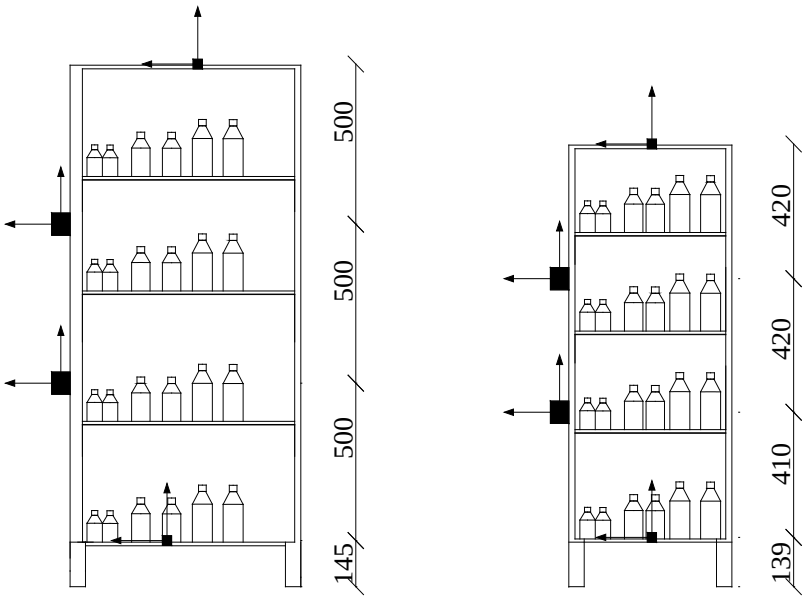

Fig. 3. Accelerometer position on the double-window cabinet (left) and the single-window cabinet (right).

3 Dynamic identification through the experimental method

3.1 *Natural frequency*

During random vibration tests, sliding between components and floors was not observed. The transfer curve method (e.g. [24, 25]) is adopted to evaluate the natural frequency of the different components. Block averaging and Hanning windowing techniques (e.g. [26], among many others) are also adopted. The length of each block, i.e. N_{FFT}, defines the resolution of the transfer curve. Moreover, a 50% block overlap is also utilized. The length of each block is adequately selected to define a fairly regular transfer curve. The method is applied for the sample cabinets and the desk. Typical transfer curves are plotted in Fig. 4. The N_{FFT} is selected equal to 1024 and to 4096 respectively for the transfer curves of the cabinets and the desk. Considering that the sampling frequency of the accelerometers is equal to 400 Hz, the frequency resolution of the transfer curve is 0.391 Hz for the cabinets and 0.098 Hz for the desk. An average transfer curve is evaluated for each test group from the gray curves corresponding to each single test. The peak in the mean transfer curve denotes the natural frequency associated to one of the vibrational modes of the tested components.

The transfer curves in Fig. 4 emphasize the presence of multiple modes of vibration. In the case of the cabinets, the high frequency peaks seem to be related to modes that involve only a limited portion of the component, e.g. window natural mode, as discussed in Section 4. The fundamental frequencies for the different random tests are summarized in Table 3. It should be emphasized that each test group included different mass distributions and different input directions. The results relative to the first three test groups should be investigated separately from the results related to the last three test groups, due to the different input motion direction on the components (see Section 2).

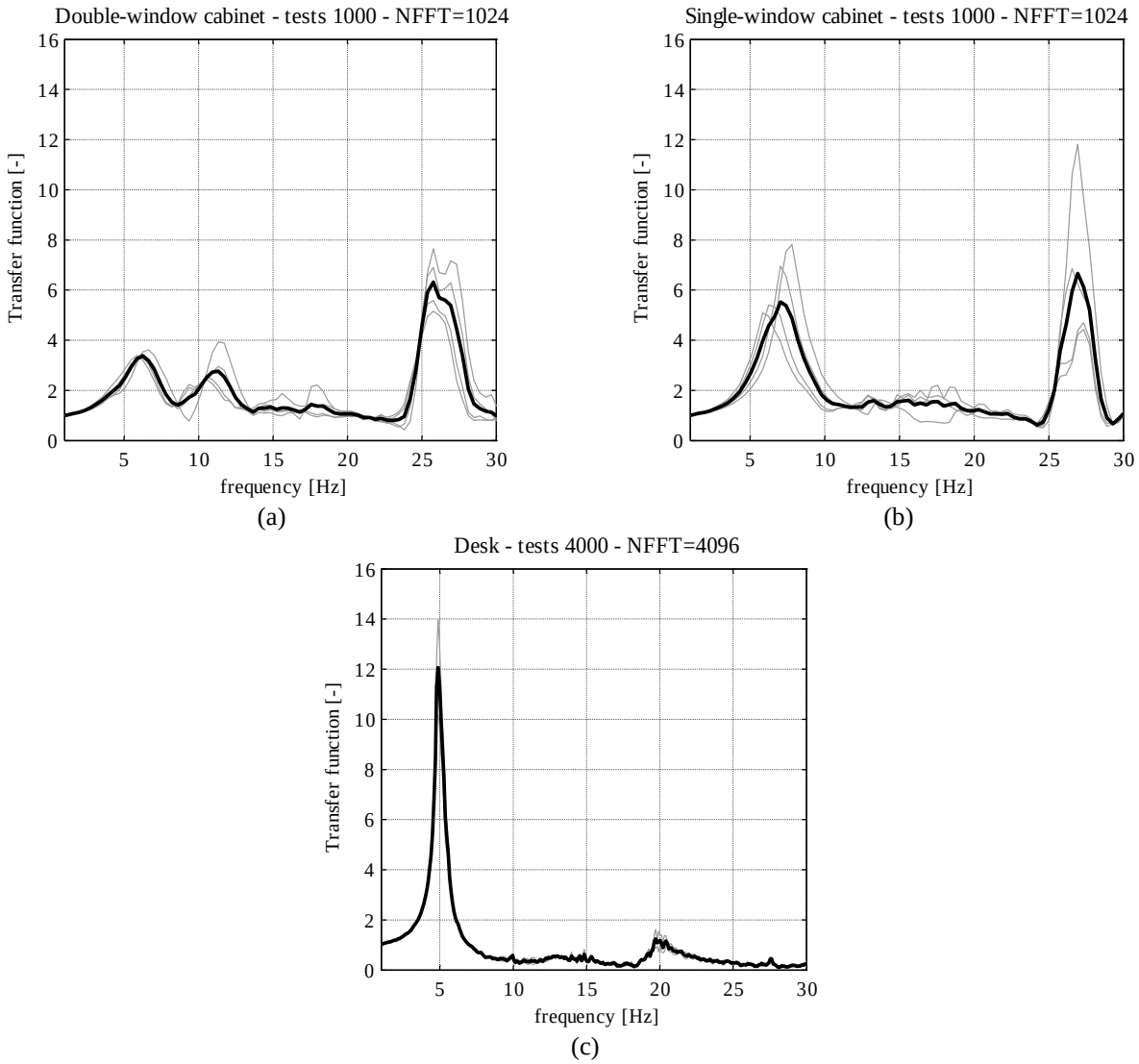

Fig. 4. Transfer curves for (a) double-window cabinet – tests 1000, (b) single-window cabinet – tests 1000, (c) desk – tests 4000. The thick curves represent the average among the tests in each group.

The short time Fourier transform method [27] is also implemented in order to evaluate the natural frequency variation during each test. In particular, for every 1 second spaced time step t, a 7 second time window centered in t is considered. The transfer curve method is applied for each time

window, defining a transfer function for each time step t. In Fig. 5 for each considered time step t, the transfer functions of the tests on the double-window cabinet are plotted in the time domain, defining a 3D plot, i.e. a spectrogram. The peak in the transfer function identifies the natural frequency of the examined component. The variation of the natural frequency within a test can be thus easily detected through this methodology.

Table 3. Fundamental frequency of the tested components for the different random test groups.

Test group ID	double-window	single-window	desk
1000	6.25 Hz	7.03 Hz	20.31 Hz
2000	5.08 Hz	6.64 Hz	20.31 Hz
3000	6.25 Hz	7.03 Hz	20.70 Hz
4000	4.68 Hz	7.03 Hz	5.08 Hz
5000	5.08 Hz	8.20 Hz	5.08 Hz
6000	4.30 Hz	7.81 Hz	5.08 Hz

Both the 3D and the contour plots of the spectrogram recorded during test no. 1001 on the double-window cabinet are shown in Fig. 5. The spectrograms recorded on the single-window cabinet and the desk during test no. 1001 and 4001, respectively, are depicted in Fig. 6.

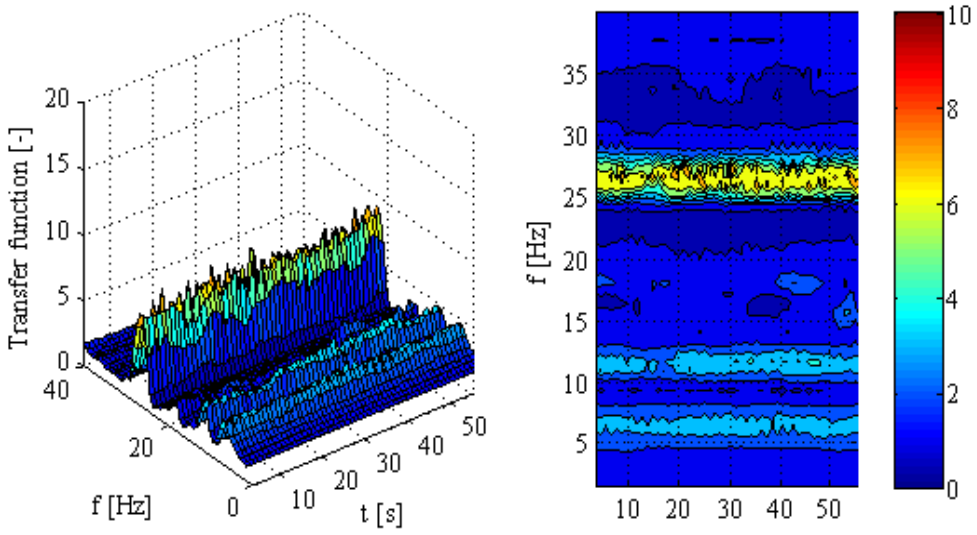

Fig. 5. 3D and contour plots of the spectrogram recorded on the double-window cabinet during test no. 1001.

The components are characterized by different natural frequencies along the two horizontal directions. Three natural modes are detected in the double-window cabinet, in case it is shaken along its transversal direction, whereas the single-window cabinet exhibits two natural modes. The results related to the desk evidence a single natural frequency; the natural frequency is slightly

larger than 20 Hz in the transversal direction and about 5 Hz in the longitudinal direction. The peak recorded in the desk is narrower than the peaks recorded in the cabinets, denoting a less damped natural mode (see Section 3.2).

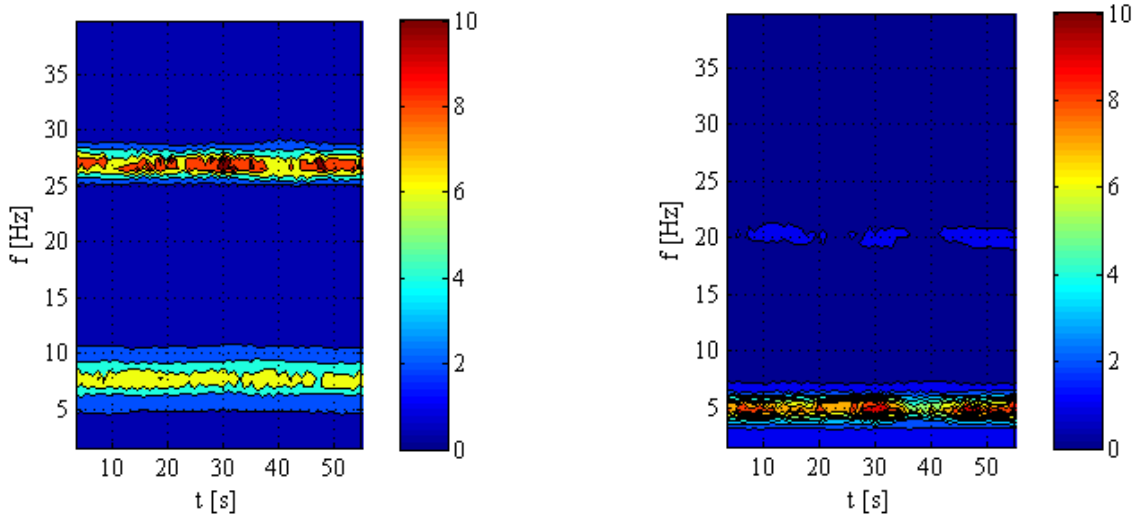

Fig. 6. Contour plots of the spectrogram (a) on the single-window cabinet during test no. 1001 and (b) on the desk during test no. 4001.

For the double-window cabinet, the natural frequency is not significantly affected by the mass amount and arrangement. It should be noted that the results related to successive test groups may be affected by the progressive damage of the components during the shakings [22]; the components are replaced only before test group 4000. The spectrogram diagrams show that negligible variations of the natural frequencies are recorded during the random vibration tests, due to the low intensity input. These experimental results will be used as benchmarks for the calibration of the numerical models of the components, reported in Section 4.

3.2 *Damping evaluation*

The damping ratio for the first mode of the two cabinets and the desk is experimentally evaluated based on the dynamic identification tests described in Section 2. The damping ratios are evaluated according to two different dynamic identification techniques through the System Identification Toolbox available in Matlab [28]: (a) Transfer Function estimation and (b) Output Error method [29]. The outcomes of the application of these techniques for a single test for the double-window cabinet, the single-window cabinet and the desk is shown in Fig. 7. The natural frequency and the

damping ratio corresponding to the natural frequency are included in the title for both the considered techniques.

It is worth mentioning that the half-power bandwidth method [24] was also employed by the Authors to compute the damping ratios. However, for the sample medical components, the latter method tends to overestimate the damping ratio due to the presence of multiple modes in a narrow frequency range. Indeed, Wang et al. [30] found that the half-power bandwidth method, which can be rigorously applied to single-degree-of-freedom (SDOF) systems, might significantly over-estimate the damping ratios of multiple-degree-of-freedom systems. The tested components exhibit a typical dynamic response of MDOF systems.

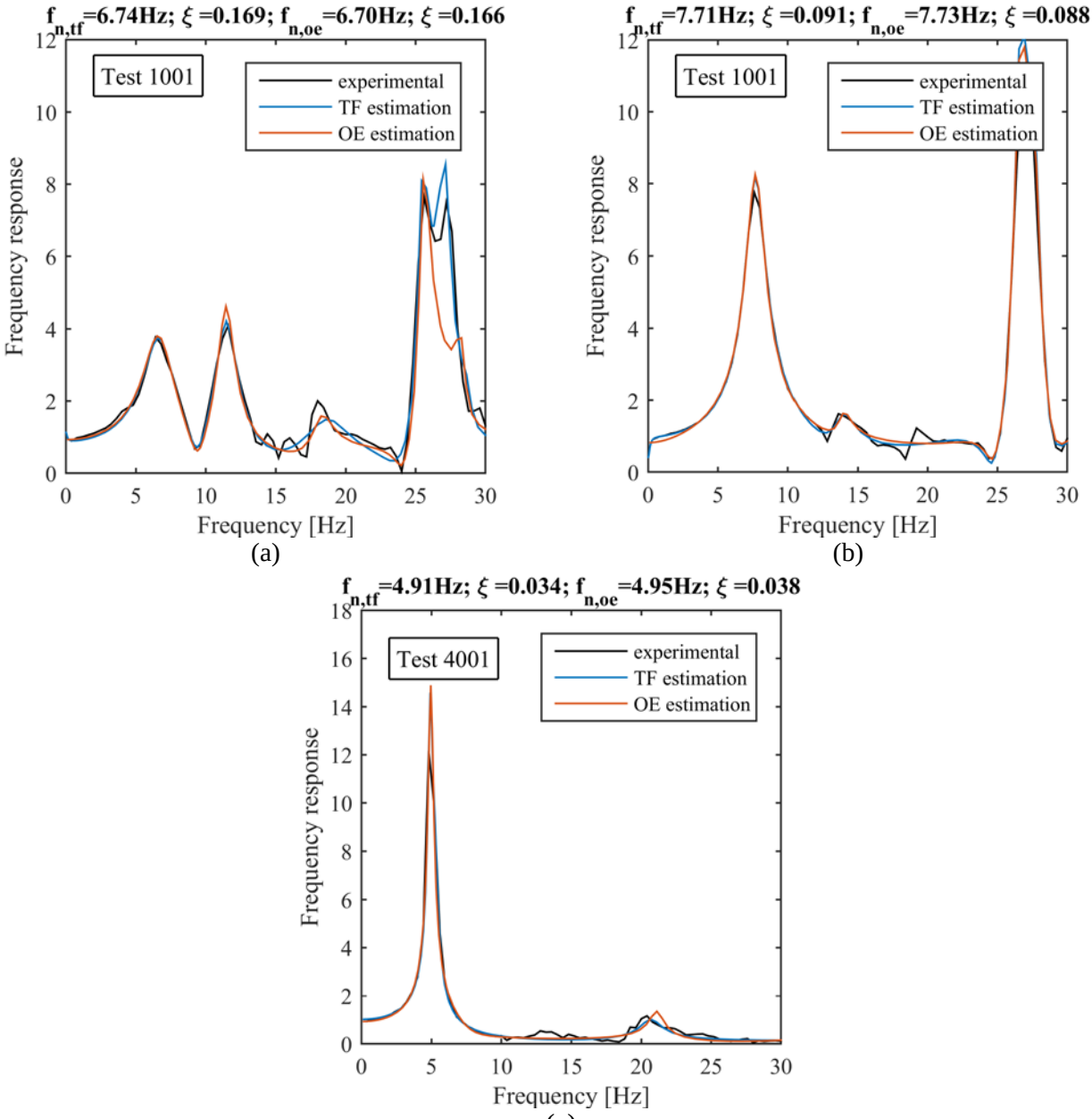

Fig. 7. Frequency response (transfer function magnitude) for (a) double-window cabinet – test 1001, (b) single-windows cabinet – test 1001 and (c) desk – tests 4001: experimental response (experimental) vs transfer function estimation (TF estimation) and output error estimation (OE estimation).

The damping ratio for each test group is evaluated as the mean value of the damping ratios of the different tests. The average damping ratio values for the three considered components are listed in Table 4. The damping ratio of the desk, which varies between 3.6% and 6.8%, is significantly smaller than the damping ratio of the two tested cabinets, which ranges between 12.1% and 21.6%. The maximum transfer function values, that occur at the natural frequency f_n, confirm the above outcome.

Table 4. Damping ratio of the tested components for the different random test groups.

Test group ID	double-window	single-window	desk
1000	17.5%	12.1%	6.8%
2000	18.8%	14.0%	4.8%
3000	14.6%	12.3%	4.9%
4000	20.6%	20.3%	4.5%
5000	16.5%	16.6%	3.6%
6000	21.6%	15.5%	3.8%

4 Numerical simulation of the components

The tested components are also simulated numerically through the Sap 2000 program [31]. The results of the finite element models are compared to the experimental data measured during the full-scale shaking table tests. An accurate survey of the different components is required in order to increase the accuracy of the numerical models.

4.1 *Desk*

The desk is composed of two tubular steel frames along its longitudinal side connected one another by four steel horizontal elements, a tubular footrest and a plywood top (Fig. 8). Moreover, a chest of drawers is screwed on the left vertical “columns” of the frames. The plywood top is 120 cm x 170 cm x 1.8 cm and it is positioned at the top of the longitudinal frames at 75 cm height. The bay of the longitudinal frames is 100.5 cm wide and the distance between the frames is 55.5 cm. Each longitudinal frame is composed of three different steel elements, i.e. two vertical elements and a horizontal one, connected each other. The tubular steel is characterized by a hollow circular cross section, whose diameter is 3.5 cm, while the thickness is 0.18 cm. The four steel elements connecting the longitudinal frames are: two 2.0 cm x 0.2 cm rectangular steel elements placed at the top of the frames and two 3.5 cm x 0.18 cm hollow circular steel elements at 16.7 cm height. The footrest, a 3.5 cm x 0.18 cm hollow circular steel element, is connected to the frame through a single-bolted connection. The chest of drawers is connected to the vertical elements of the frames by a bolt at 4 different positions, i.e. two connections are located at 21 cm from the floor and the other two ones at 46 cm from the floor; the chest of drawers dimensions are 58 cm x 37 cm x 29 cm

(height). The mass of the steel elements is 12.2 kg, while the mass of the drawers is 11.4 kg and the mass of the plywood top is 8.0 kg.

The desk is modelled assuming a base restrained with four hinges. The footrest has rotation releases that simulate the single-bolt connection. The connection between the vertical and horizontal elements of the longitudinal frames is characterized by a rotational stiffness equal to 2.2 kNm/rad. Such a stiffness models the partial constraint given by the tube-to-tube connection depicted in Fig. 8.

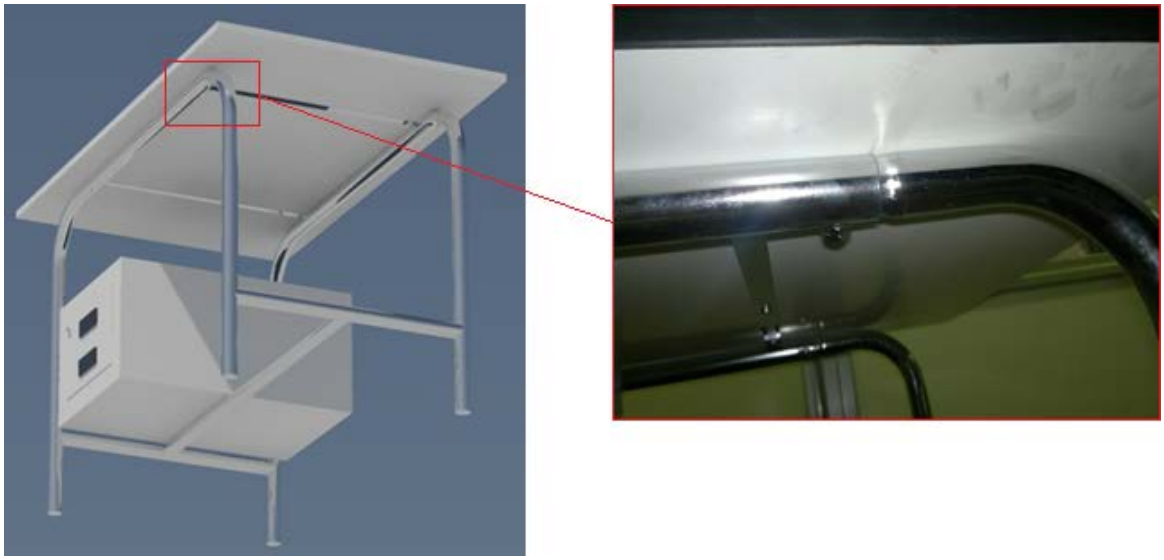

Fig. 8. Tube-to-tube connection between the steel elements of the desk.

The stiffness value is calibrated in order to have a good experimental-to-numerical matching. Indeed, in case such a connection is modelled through a fixed restraint, the natural frequency can increase up to 3 times, i.e. from 4.9 Hz to 13.6 Hz. The accurate estimation of the stiffness of tube-to-tube connection assumes therefore a key role in the evaluation of the dynamic properties of the desk.

The presence of the plywood top is modelled through the addition of four 2 kg masses applied at the top of the desk. The nodes of the longitudinal frame where the desk is screwed are constrained with body constraints. The chest of drawers is modelled with four 2.85 kg masses applied at the connection points between the chest and the longitudinal frame. A body constraint is imposed among these four points. Finally, the steel elements are modeled with a distributed mass and they are characterized by a 210000 N/mm^2 elastic modulus. Modal analyses show a first mode frequency

equal to 4.9 Hz and a second mode frequency equal to 22.6 Hz (Fig. 9). The first mode shape denotes a pure translation in the longitudinal direction of the desk, while the second mode shape evidences a coupled motion in the transversal direction, due to the presence of the chest of drawers.

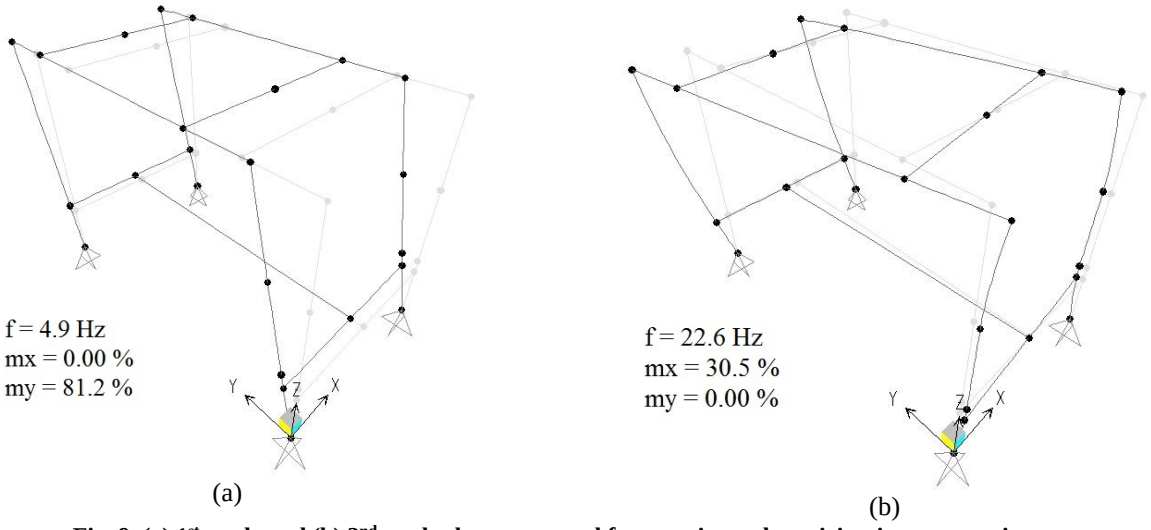

Fig. 9. (a) 1st mode and (b) 2nd mode shapes, natural frequencies and participating mass ratios.

The FEM results give a fairly good matching with the experimental results (Table 3), considering that a very close match is outside the scope of the paper. The experimental tests highlight significant variations in terms of natural frequency in case the component is shaken along the two horizontal directions. The comparison is clearly evidenced in Table 5.

Table 5. Comparison between the natural frequencies resulting from the FEM analysis and the transfer curve.

Shaking Direction	Longitudinal	Transversal
FEM	4.9 Hz	22.6 Hz
Transfer curve	5.1 Hz	20.7 Hz

4.2 *Cabinets*

The cabinets are composed of four steel vertical columns connected each other by steel elements. The global dimensions of both the investigated cabinets are summarized in Table 6.

Table 6. Dimensions of the investigated cabinets.

	height [cm]	width [cm]	depth [cm]
Double-window cabinet	165	74.5	38
Single-window cabinet	139	53	36

The vertical steel elements are characterized by an angular 55 cm x 50 cm “L” section with 0.1 cm thickness, with the 55 mm wide flange parallel to the transversal side of the cabinet. They are

connected by two steel horizontal plates with side stiffeners and bolted connections, at the top of the cabinet and at 17 cm height (Fig. 10). The steel plates and their stiffeners are characterized by 1 mm thickness, whereas the stiffeners are 3.0 cm high. Three of the four vertical bays are infilled with 1 mm thick steel plates, whereas glass windows are installed in the fourth bay. The double-window cabinet is also characterized by a 5 cm x 0.1 cm rectangular vertical steel element that separates the two glass windows.

(a) (b)

Fig. 10. Global view of the sample cabinets.

4.2.1 Single-window cabinet

The vertical steel columns are modelled according to their actual geometry. The presence of the steel horizontal plates is modelled through four horizontal steel elements characterized by a 0.1 cm (width) x 3 cm (height) rectangular cross section both at the top and at 17 cm height of the cabinet. These horizontal elements are characterized by a large out-of-plane stiffness, i.e. large moment of inertia about the vertical axis, to simulate the presence of the steel horizontal plate element. Furthermore, two diaphragm constraints are imposed between the 4 points at the top and the 4 points at 17 cm height. The vertical panels are not included in the model, since they are connected so as not to increase the lateral stiffness of the cabinet. The glass window is modelled with a properly meshed shell element, assuming a 80000 N/mm^2 elastic modulus. Hence, the adopted model is able to capture both the global modes in the two horizontal directions, which involve the

whole cabinet, and the local ones, which involve a portion of the cabinet. Rigid elements in the out-of-plane direction are included between the steel elements and the glass window in order to model the restraint given by their connection (Fig. 11), whereas the glass window does not contribute to the in-plane stiffness; indeed, the glass window is connected to the cabinet only along one of the two vertical sides. A rigid element in the out of plane direction is also included to model the lock of the glass window.

Fig. 11. Connection between the steel elements and the glass window of the single-window cabinet.

The single-window cabinet mass is 15 kg, excluding the window mass; for the sake of simplicity, the mass is equally divided between the top and the base of the cabinet. The steel elements are characterized by no mass, whereas the mass is included in the glass window in order to correctly estimate the local vibrational modes of the glass window. Different mass amounts are inserted at the shelf levels, according to the actual mass adopted in the experimental phase for the different test groups. In Fig. 12 the modal shapes of the single-window cabinet for the test group 1000 are depicted. The first and the second vibrational modes are represented in Fig. 12a and in Fig. 12b respectively, whose frequencies are 6.18 Hz and 7.38 Hz. In Fig. 12c a local mode that involves the glass window is represented.

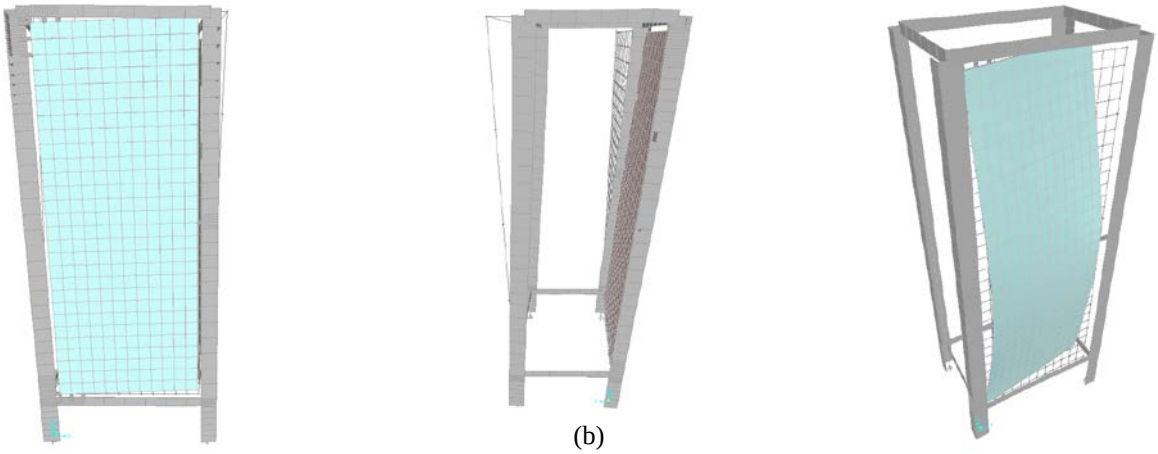

(a) (b) (c)

Fig. 12. Single-window cabinet modal shapes in tests 1000 and 4000: (a) I vibration mode (6.18 Hz), (b) II vibration mode (7.38 Hz), (c) III vibration mode (23.12 Hz).

The FEM results give a fairly good matching with the transfer curve represented in Fig. 4b, considering that a very close match is outside the scope of the paper. The peak represented in the transfer curve, which occurs at 26 Hz, is compatible with the frequency of the local mode in the FEM model. The comparison between the numerical and the experimental natural frequencies for the different test groups is summarized in Table 7.

Table 7. Comparison between the frequency results from the FEM analysis and the transfer curve.

Test group	FEM model	Experiment	Δ [%]
1000	7.38 Hz	7.03 Hz	+5.0
2000	8.84 Hz	6.64 Hz	+33.1
3000	8.21 Hz	7.03 Hz	16.8
4000	6.18 Hz	7.03 Hz	-12.1
5000	7.64 Hz	8.20 Hz	-6.8
6000	7.09 Hz	7.81 Hz	-9.2

The numerical and the experimental frequencies of the tested cabinet are close. Considering the low level of accuracy of the model with respect to the complexity of the geometry and the mechanical connections between the elements, the outcomes of the numerical analyses give a good approximation of the experimental ones. It is therefore demonstrated that simple models are able to capture the dynamic properties of the tested cabinet.

4.2.2 Double-window cabinet

The modelling approach of the double-window cabinet is very similar to the one provided for the single-window cabinet. However, the dimension and the mass, i.e. 20 kg, are slightly different than the corresponding values in the single-window cabinet. The vertical steel element between the two windows is properly modelled according to its own geometry; such an element is hinged to the cabinet, in order to model the single-bolted connection. The connection between the cabinet and glass window is modelled by rigid elements in the out of plane direction, similarly to the single-window cabinet. The rigid elements simulate the actual restraints given to the glass window by a steel connector. The different mass amounts corresponding to the different performed test groups are inserted at the shelf levels. In Fig. 13 the modal shapes of the double-window cabinet for the test group 1000 are shown. The first four natural modes are included: the first two modes involve the whole cabinet, the third one is a local mode that involves the vertical element between the two glass windows and the fourth mode involves the glass windows.

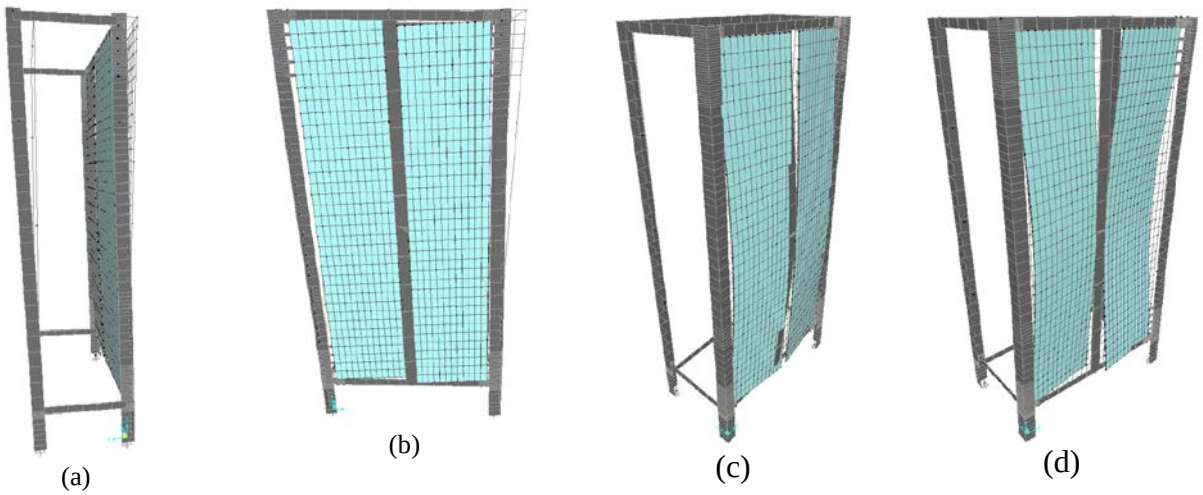

Fig. 13. Double-window cabinet modal shapes in tests 1000 and 4000: (a) I vibration mode (4.74 Hz), (b) II vibration mode (5.08 Hz), (c) III vibration mode (10.35 Hz), (d) IV vibration mode (19.90 Hz).

The FEM outcomes give a fairly good matching with the transfer curve represented in Fig. 4a. The three peaks represented in the transfer curve, which occur at about 6 Hz, 11 Hz and 25 Hz, respectively, are compatible with the frequencies of the first, third and fourth modes in the FEM model. In particular, the numerical model allows justifying the differences in the transfer curves among the single- and the double-window cabinets. Indeed, the double-window transfer curve

denotes three evident peaks, whereas the single-window one exhibits only two peaks. The comparison between the numerical and the experimental natural frequencies for the different test groups is summarized in Table 8.

Table 8. Comparison between the frequency results from the FEM analysis and the transfer curve.

Test group	FEM model	Experiment	Δ [%]
1000	5.08 Hz	6.25 Hz	-18.7
2000	5.57 Hz	5.08 Hz	+9.6
3000	5.30 Hz	6.25 Hz	-15.2
4000	4.74 Hz	4.68 Hz	+1.3
5000	5.40 Hz	5.08 Hz	+6.3
6000	5.04 Hz	4.30 Hz	+17.2

Also for the double-window cabinet, the numerical and the experimental frequencies of the tested cabinet are in similar ranges. It can be concluded that simple models are able to simulate reliably the dynamic properties of the cabinets.

4.3 *Numerical vs experimental results: mode shapes and transfer curves*

The accuracy of the simple models defined in the previous paragraphs is assessed through the numerical-to-experimental comparison of the transfer curves and mode shapes.

In order to compare the numerical transfer curves with the experimental ones, a time-history linear analysis is performed in SAP 2000 [31] on the three sample components. The recorded accelerations at the shake table level are selected as input at the base of the components. The damping ratio is set equal to the damping ratio assessed through the half-bandwidth method.

The numerical transfer curves between the base and the top of the components are compared to the experimental transfer curves (Fig. 14). A fairly good matching is observed, considering the simplicity of the adopted models.

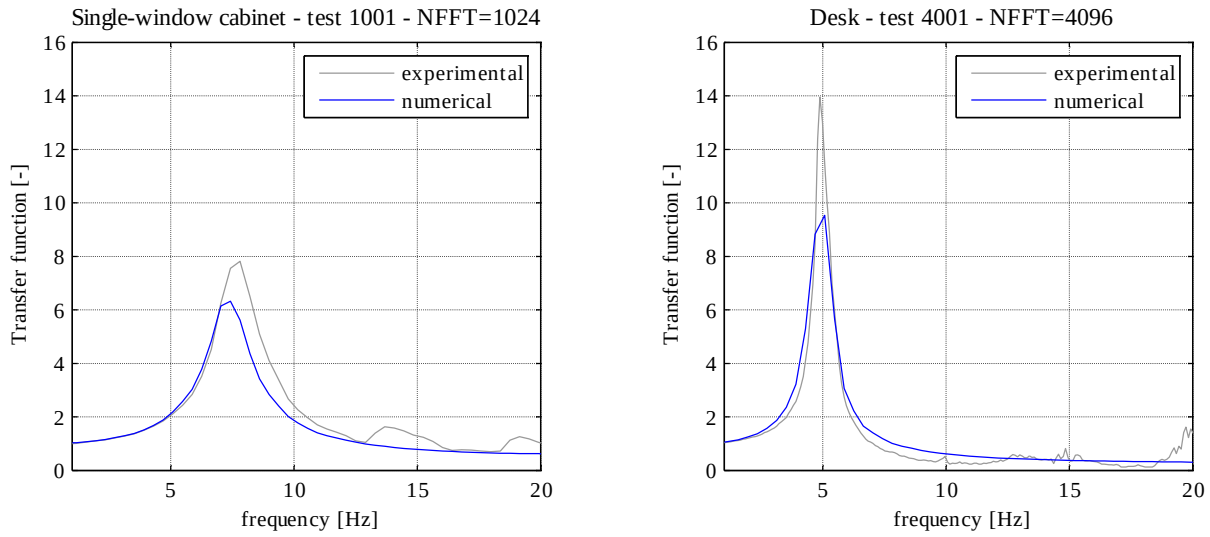

Fig. 14. Numerical vs experimental transfer curves between the top and the base of (a) the single-window cabinet in test 1001 and (b) the desk in test 4001.

The transfer function at different levels of the cabinets are employed to assess the experimental mode shapes of the cabinets. Towards this aim, it is assumed that the ratio of the story transfer function magnitudes at the natural frequency is equal to the ratio of the mode shape [24]. The transfer functions are therefore evaluated between the base of the cabinets and the locations where the different accelerometers are positioned (Fig. 3). The random tests 1004 and 4002 are adopted for the evaluation of the mode shapes in the transversal and longitudinal directions, respectively. The mode shapes are then compared in both the orthogonal directions (Table 9). The modal assurance criterion (MAC) [32] may be utilized to pair mode shapes derived from numerical models and test measurements. The MAC value between a measured mode and an numerical mode is defined as a scalar constant and provides a measure of the least squares deviation or 'scatter' of the points from the straight line correlation. The MAC values for the considered components are close to the unity; in particular, they are equal to 0.968 and 0.962 for the 1st and 2nd modes of the single-window cabinets included in Table 9. These results are in agreement with the previous ones; they demonstrate that simple models are able to simulate the dynamic response of the sample nonstructural components.

412 **Table 9. Mode shapes of the single-window cabinet.**

	1st mode – longitudinal direction		2nd mode – transversal direction	
Height [cm]	numerical	experimental	numerical	experimental
13.9	0.094	0.298	0.091	0.251
54.9	0.394	0.488	0.414	0.354
96.9	0.716	0.639	0.744	0.534
138.9	1.000	1.000	1.000	1.000

413

414 # 5 Conclusions

415 The outcomes of a comprehensive shake table test program, aimed at investigating the dynamic
416 response of typical components of a consultation room in hospital buildings, are illustrated in the
417 present paper. Low-intensity random vibration tests are carried out on two freestanding medical
418 cabinets and a desk. Different mass configurations distributed along the height of the cabinets are
419 considered. The modal response quantities of the components, namely the natural frequency and the
420 damping ratio, are investigated via standardized methods.

421 The transfer curve method emphasizes the occurrence of multiple modes of vibration of the
422 components. The desk is characterized by a significantly different natural frequency along the two
423 horizontal directions. The damping ratio is estimated through the half-power bandwidth
424 methodology. The damping ratio of the desk varies between 3.6% and 6.8%, whereas the damping
425 ratio of the two tested cabinets, which ranges between 12.1% and 21.6%, is significantly high.

426 Simplified yet reliable finite element models of the experimentally tested sample components are
427 defined upon the laboratory outcomes through the computer platform routinely used for practical
428 applications. The natural frequencies of the numerical model of the desk match the experimental
429 results. The numerical model implemented is capable to simulate the variations of natural frequency
430 as provided by the experimental tests, in case the component is shaken along the two horizontal
431 directions. The natural modes of the two tested cabinets are adequately simulated by the numerical
432 model. The multiple peaks observed in the transfer curves are associated to a mode shape. The
433 dynamic response of the defined models is assessed through the numerical-to-experimental

comparison of the transfer curves and mode shapes. Considering the low level of accuracy of the model with respect to the complexity of the components, the outcomes of the numerical analyses provide a close approximation of the experimental ones. The main finding of the present numerical study is therefore that simple models are able to adequately simulate the dynamic properties of the tested cabinets. The developments provided in this study could be easily used by inspectors facing the problem of evaluating the seismic risk of nonstructural components in hospital buildings; additional reliable yet sound guidelines are still under investigation by the authors. Furthermore, the developed models can be easily used to assess the seismic demand on such components corresponding to a given base input motion; for instance, they can indicate the need to restrain the cabinet at their base.

Finally, it is emphasized that the outcomes related to the developed models is limited to freestanding components which do not exhibit any rocking mechanism, i.e. they are rigidly connected at their base to the floor.

Acknowledgements

The research study presented in the present paper has been funded by the Italian Department of Civil Protection in the frame of the national projects DPC - ReLUIS 2010-2013, Task 2.2.2, Vulnerability and risk assessment of health care facilities and DPC-ReLUIS 2014, RS9 Health Care Facilities. The authors would like to acknowledge Siniat that provided the ceiling and the partitions used in the testing program. The insightful discussions with Dr. G. Maddaloni, who assisted with the full scale shaking-table tests, are also fully appreciated. The authors would also like to thank the three anonymous reviewers for their insightful comments and suggestions.

References

[1] Taghavi S, Miranda E. Response assessment of nonstructural building elements, PEER report 2003/05. College of Engineering, University of California Berkeley, USA 2003.

[2] Filiatrault A, Uang CM, Folz B, Christopoulos C, Gatto K. Reconnaissance report of Nisqually (Seattle-Olympia) February 28, 2001 Earthquake. Report No.SSRP-2001/2002. Department of Structureal Engineering, University of California San Diego. La Jolla, CA. 2001.

[3] Kircher CA. It makes dollars and sense to improve nonstructural system performance. ATC 29-2 Seminar on Seismic Design, Performance and Retrofit of Nonstructural Components in Critical Facilities, Newport Beach, CA 2003.

[4] Maffei J, Bazzurro P. The 2002 Molise, Italy, Earthquake. Earthq Spectra. 2004;20:S1-S22.

[5] Price HJ, De Sortis A, Schotanus M. Performance of the San Salvatore Regional Hospital in the 2009 L'Aquila Earthquake. Earthq Spectra. 2012;28:239-56.

[6] Mitrani-Reiser J, Mahoney M, Holmes WT, de la Llera JC, Bissell R, Kirsch T. A Functional Loss Assessment of a Hospital System in the Bío-Bío Province. Earthq Spectra. 2012;28:S473-S502.
[7] Di Sarno L, Yenidogan C, Erdik M. Field evidence and numerical investigation of the Mw= 7.1 October 23 Van, Tabanlı and the Mw> 5.7 November earthquakes of 2011. Bull Earthq Eng. 2013;11:313-46.
[8] Masi A, Santarsiero G, Gallipoli M, Mucciarelli M, Manfredi V, Dusi A et al. Performance of the health facilities during the 2012 Emilia (Italy) earthquake and analysis of the Mirandola hospital case study. Bull Earthq Eng. 2013:1-25.
[9] Rojahn C, Maffei JR, Basso RA, Bearzi V, De Sortis A, Di Pasquale G et al. Recommended U.S.-Italy Collaborative Guidelines for Bracing and Anchoring Nonstructural Components in Italian Hospitals. ATC-51-2. Applied Technology Council, Redwood City, California 2004.
[10] CEN. Eurocode 8: design of structures for earthquake resistance - Part 1: general rules, seismic actions and rules for buildings. EN 1998-1. Brussels, Belgium. 2004.
[11] American Society of Civil Engineers. ASCE/SEI 7-10: Minimum Design Loads for Buildings and Other Structures. Reston, Virginia, US 2010.
[12] Building Standard Law of Japan. 2000.
[13] New Zealand Standards (NZS). Structural Design Actions. Earthquake Actions - NZS 1170.5. Wellington, New Zealand 2004.
[14] Konstantinidis D, Makris N. Experimental and analytical studies on the response of freestanding laboratory equipment to earthquake shaking. Earthq Eng Struct Dyn. 2009;38:827-48.
[15] Lopez Garcia D, Soong TT. Sliding fragility of block-type non-structural components. Part 1: Unrestrained components. Earthq Eng Struct Dyn. 2003;32:111-29.
[16] Hutchinson TC, Chaudhuri SR. Bench-shelf system dynamic characteristics and their effects on equipment and contents. Earthq Eng Struct Dyn. 2006;35:1631-51.
[17] Shenton HW. Criteria for initiation of slide, rock, and slide-rock rigid-body modes. J Eng Mech-Asce. 1996;122:690-3.
[18] Consiglio Superiore dei Lavori Pubblici. Decreto Ministeriale del 14/01/2008, Approvazione delle nuove norme tecniche per le costruzioni. G.U. n. 29 del 4/2/2008 (in Italian) 2008.
[19] Kuo K-C, Suzuki Y, Katsuragi S, Yao GC. Shake table tests on clutter levels of typical medicine shelves and contents subjected to earthquakes. Earthq Eng Struct Dyn. 2011;40:1367-86.
[20] Sato E, Furukawa S, Kakehi A, Nakashima M. Full-scale shaking table test for examination of safety and functionality of base-isolated medical facilities. Earthq Eng Struct Dyn. 2011;40:1435-53.
[21] Magliulo G, Pentangelo V, Maddaloni G, Capozzi V, Petrone C, Lopez P et al. Shake table tests for seismic assessment of suspended continuous ceilings. Bull Earthq Eng. 2012;10:1819-32.
[22] Cosenza E, Di Sarno L, Maddaloni G, Magliulo G, Petrone C, Prota A. Shake table tests for the seismic fragility evaluation of hospital rooms. Earthq Eng Struct Dyn. 2014;44:23-40.
[23] FEMA 461. Interim Testing Protocols for Determining the Seismic Performance Characteristics of Structural and Nonstructural Components. Redwood City, California, USA 2007.
[24] Bracci JM, Reinhorn AM, Mander JB. Seismic resistance of Reinforced Concrete Frame Structures Designed Only for Gravity Loads: Part I - Design and Properties of a One-Third Scale Model Structure. Technical Report NCEER-92-0027. State University of New York at Buffalo, NY, US 1992.
[25] Magliulo G, Petrone C, Capozzi V, Maddaloni G, Lopez P, Talamonti R et al. Shake Table Tests on Infill Plasterboard Partitions. Open Constr Build Technol J. 2012;6:155-63.
[26] Proakis JG, Monalakis DG. Digital Signal Processing: Principles, Algorithms and Applications. Pearson Prentice Hall, New Jersey, NY 2007.
[27] Gabor D. Theory of communications. J Inst Elect Eng. 1946;93:429-57.
[28] The MathWorks Inc. MATLAB Release 2015a. Natick, Massachusetts, United States 2015.
[29] Ljung L, Glac T. Modeling of Dynamic Systems: Prentice Hall; 1994.

[30] Wang J-T, Jin F, Zhang C-H. Estimation error of the half-power bandwidth method in identifying damping for multi-DOF systems. Soil Dyn Earthq Eng. 2012;39:138-42.
[31] CSI Computer & Structures Inc. SAP2000. Linear and Nonlinear Static and Dynamic Analysis of Three-Dimensional Structures, Computer & Structures, Inc. Berkeley, California 2004.
[32] Allemang RJ. The modal assurance criterion - Twenty years of use and abuse. Sound Vib. 2003;37:14-23.

List of figures

Fig. 1. Single-window cabinet in (a) test groups 1000 and 4000, (b) test groups 2000 and 5000 and in (c) test groups 3000 and 6000. 6
Fig. 2. Photo and plan view of the test setup: (a) and (c) configuration 1, adopted in test groups 1000, 2000 and 3000, and (b) and (d) configuration 2, adopted in test groups 4000, 5000 and 6000. 7
Fig. 3. Accelerometer position on the double-window cabinet (left) and the single-window cabinet (right). 9
Fig. 4. Transfer curves for (a) double-window cabinet – tests 1000, (b) single-window cabinet – tests 1000, ... 10
Fig. 5. 3D and contour plots of the spectrogram recorded on the double-window cabinet during test no. 1001. 11
Fig. 6. Contour plots of the spectrogram (a) on the single-window cabinet during test no. 1001 and (b) on the desk during test no. 4001. 12
Fig. 7. Frequency response (transfer function magnitude) for (a) double-window cabinet – test 1001, (b) single-windows cabinet – test 1001 and (c) desk – tests 4001: experimental response (experimental) vs transfer function estimation (TF estimation) and output error estimation (OE estimation). 14
Fig. 8. Tube-to-tube connection between the steel elements of the desk. 16
Fig. 9. (a) 1st mode and (b) 2nd mode shapes, natural frequencies and participating mass ratios. 17
Fig. 10. Global view of the sample cabinets. 18
Fig. 11. Connection between the steel elements and the glass window of the single-window cabinet. 19
Fig. 12. Single-window cabinet modal shapes in tests 1000 and 4000: (a) I vibration mode (6.18 Hz), (b) II vibration mode (7.38 Hz), (c) III vibration mode (23.12 Hz). 20
Fig. 13. Double-window cabinet modal shapes in tests 1000 and 4000: (a) I vibration mode (4.74 Hz), (b) II vibration mode (5.08 Hz), (c) III vibration mode (10.35 Hz), (d) IV vibration mode (19.90 Hz). 21
Fig. 14. Numerical vs experimental transfer curves between the top and the base of (a) the single-window cabinet in test 1001 and (b) the desk in test 4001. 23

List of tables

Table 1. Test program details. 6
Table 2. Random vibration tests ID, acceleration amplitude and root mean square. 8
Table 3. Fundamental frequency of the tested components for the different random test groups. 11
Table 4. Damping ratio of the tested components for the different random test groups. 15
Table 5. Comparison between the natural frequencies resulting from the FEM analysis and the transfer curve. 17
Table 6. Dimensions of the investigated cabinets. 17
Table 7. Comparison between the frequency results from the FEM analysis and the transfer curve. 20
Table 8. Comparison between the frequency results from the FEM analysis and the transfer curve. 22
Table 9. Mode shapes of the single-window cabinet. 24